

Fabrication, Microstructure and Properties of Mechanically Alloyed and Electrochemically Etched Porous Ti-Y₂O₃

Montasser Dewidar¹, G. Adamek², J. Jakubowicz², and Khalil AbdelRazik Khalil^{1,3,*}

¹ Department of Materials and Mechanical Design, Faculty of Energy Engineering, Aswan University, Aswan, Egypt.

² Poznan University of Technology, Institute of Materials Science and Engineering, M. Sklodowska-Curie 5 Sq., 60-965 Poznan, Poland

³ King Saud University, Department of Mechanical Engineering, College of Engineering, P.O. Box 800, Riyadh 11421, Saudi Arabia.

*E-mail: kabdelmawgoud@KSU.EDU.SA

Received: 27 July 2014 / Accepted: 11 October 2014 / Published: 28 October 2014

In this study the formation of porous Ti-10wt.%Y₂O₃ nanostructure biomaterial was described. After high-energy ball milling of a Ti-Y₂O₃ for 24 h, powder mixture was pressed and sintered to consolidate the granules. Mechanically alloyed Ti-Y₂O₃ has nanostructure with grain size in the range of 150 nm and large grain boundaries volume fraction, which essentially to improve etching process. The sintered compacts were electrochemically etched in a mixture of H₃PO₄ and HF electrolyte at 10 V for 25 min. The electrolyte penetrates sintered samples through the grain boundaries, resulting in effective material removing and pores formation. The pore diameter reaches up to 50 μm, which is very attractive for strong bonding with bone. The ultra low grain size structure improves mechanical properties of the implants in comparison to commonly used microcrystalline Ti-based implants. The corrosion properties were investigated in Ringer's solution. Mechanically alloyed samples followed by electrochemical etching shows good corrosion resistance.

Keywords; Mechanical alloying; Nanocomposite; Mechanical properties, Corrosion.

1. INTRODUCTION

There is a high seeks for biomaterials to assist the replacement of organs and their functions. Interaction between biomaterial and natural tissue is a significant subject for biomedical science and essential to aid the design and fabrication new biocompatible and bioactive materials. For this reason, researchers search for new biomaterials with advanced mechanical and biological properties and develop new technologies for these properties enhancement. The development of nanocomposites has emerged as an important step in creating a new generation of materials [1-4].

Among all metallic biomaterials used for bone replacement, titanium (Ti) and some of its alloys are recognized as the most successful materials for this purpose. Pure Ti or Ti-6Al-4V alloy, show very unique properties, which allow them to be used for biomedical applications. Ti based alloys have low density, high strength, no toxicity for the human body (avoiding cytotoxic metals, or reducing their amounts), good biocompatibility, and good and easy formation/processing [5-7]. Despite these advantages, there are four problems of titanium and its alloys in bone tissue application. First, the mismatch of Young's modulus between titanium materials and bones can cause severe "stress shielding", which can lead to bone resorption and eventual loosening of the implants [8]. To overcome this drawback, implant materials with porous structure have been introduced. The porous structure materials can permit the ingrowth of the new-bone tissues and the transport of the body fluids, and eventually prolong the life time [9]. Second, Ti and its alloys are essentially bioinert materials and after implanted in the living body they are merely encapsulated by fibrous tissue. As a result, they are isolated from the surrounding tissue. To solve this problem, a strong interface bonding between implants and living bones tissue is strongly required [10]. Third, Ti has insufficient corrosion resistance for long term implants. Fourth, Ti has low hardness and wear resistance [11, 12]. The ideal bone substitute is not a material that interacts as little as possible with the surrounding tissues, but one that will form a secure bond with the tissues by allowing new cells to grow. One way of achieving this is to use a porous material, so that new tissue, and ultimately new bone, can grow into the pores and help to prevent loosening and movement of the implant [13]. Also a good mechanical properties and corrosion resistance are very important factors for biomaterials.

Addition of some alloy elements and hard compound powders and mechanical alloying is an effective approach to increase mechanical properties and hardness of Ti [14-16]. However, up to now, no report has been found by adding Y_2O_3 to Ti. Based on these considerations, Ti with high hardness and good corrosion resistance could be possibly fabricated by Y_2O_3 addition using mechanical alloying and sintering method followed by electrochemical etching. In this work, we show the formation of the nanocomposite/ultrafine Ti-based alloys with Y_2O_3 additions and surface modification by electrochemical etching, which could be potentially used in hard tissue engineering.

2. EXPERIMENTAL PROCEDURES

Ti powder with average particle size 40 μm was supplied by Se-Jong Materials Ltd., Korea. Fine powder of Y_2O_3 with high purity mean particle size: 2 μm , was purchased from UBE Industries Ltd., Tokyo, Japan. The amount of Ti powder and Y_2O_3 was calculated and weighted using balance with 0.001 g accuracy. Specimens with fraction of 10 wt.% Y_2O_3 were prepared. The mechanical alloying process was applied for the preparation of the nanocomposite Ti and Y_2O_3 composite. In the mechanical alloying, pure elemental powders of Ti with additions of 10 wt.% Y_2O_3 were mechanically milled in the protective high purity argon atmosphere for 24 h using SPEX 8000 mill.

A ball-to-powder mass ratio of 30:1 by steel balls with a diameter of 20mm was employed. Milling was conducted at a rotational speed of 300 rpm. After the milling process, the powders which have grain size reaches a value of about 30-60 nm were handled in MBraun Labmaster glove box with

the automatically controlled argon atmosphere inside. The milled nanocomposites powders were cold isostatically pressed in a cylindrical mould with 400 MPa pressure using a uniaxial press machine. The green bodies have diameter of ϕ 8 mm and height of around 5 mm. All samples were then sintered in vacuum (the pressure is 20 millitorr) at 1200°C for 60 min and cooled down in the furnace to room temperature. Sintering results in density of about 80% of the theoretical value.

The Solartron 1285 potentiostat was applied in the electrochemical etching stage followed at 10V 30 min⁻¹ in 1M H₃PO₄ + 2% HF electrolyte. The properties related to the porosity were measured using Micrometrics ASAP 2020 Analyzer. Microstructure and morphology were characterized by XRD, TEM and SEM.

Corrosion resistance was measured using potentiodynamic mode in EG&G corrosion cell, with scan rate fixed to 0.5 mV/s. Ringer's solution (NaCl – 9 g/l, KCl – 0.42 g/l, CaCl₂ – 0.48 g/l, NaHCO₃– 0.2 g/l) was used as the simulated body fluids.

3. RESULTS AND DISCUSSIONS

Mechanical alloying is a process for nanomaterials synthesis. It is a solid-state powder processing technique involving repeated welding, fracturing, and rewelding of powder particles in a high-energy ball mill. In this process, the mixture of microcrystalline pure Ti elemental and Y₂O₃ powders in the stoichiometric ratio was milled for 24 h to achieve Ti-Y₂O₃ alloy composition. The typical XRD patterns of the mixture of Ti and 10 wt.% Y₂O₃ before mechanical alloying is shown in Fig 1. a. During mechanical alloying process the original sharp diffraction lines of the Ti and Y₂O₃ gradually become broader and their intensity decreases with milling time 12 h (Fig 1. b) and 24 h (Fig 1. c) respectively. Because of the fact that during milling the powder particles are subjected to severe plastic deformation, the high density of defects and consequently the disordered solid solutions are generated.

In the mechanical alloying process the starting elemental powders usually agglomerate at the early stage of milling to form powder particles of greater diameters, as large as several hundred microns, and this is followed by continuous disintegration until the particle size is less than a few microns. During mechanical alloying the powder Ti and Y₂O₃ particles are subjected to severe plastic deformation and extreme cold working. The dislocation density increases to considerably high levels and shear bands containing a high dislocation density are formed. Due to the successive accumulation of the dislocation density, the crystals are disintegrated into subgrains that are initially separated by low-angle grain boundaries. The formation of these subgrains is attributed to the decrease of the atomic level strain. After sufficient milling times, the transformation of the low-angle grain boundaries into those of the high-angle takes place by grain rotation, developing the ultrafine structures. Further ball milling time leads to further deformation occurring in the shear bands located in the unstrained parts of the powders which leads to subgrain size reduction so that the orientation of final grains becomes random in crystallographic orientations of the numerous grains and hence, the direction of slip varies from one grain to another [17].

In the presence of Y_2O_3 , a high percentage of Y_2O_3 (10 wt.%) particles infuses into the structure by diffusing down to dislocations and grain boundaries. The diffused Y_2O_3 particles are segregated into dislocations and grain boundaries. This phenomenon contributes to the fixing of dislocations and the stabilizing of grain boundaries. Afterward, the trickling down of running dislocations on the fixed dislocations leads to the nucleation of new boundaries. After milling the microcrystalline powder to 24 h, the Ti- Y_2O_3 mixture was ultra fine powders and the amorphous phase was formed directly from the starting mixture. This results in a rapid grain refinement in the order of a few nanometers. As the milling duration develops, the content fraction of such intermediate compounds increases leading to a final product which properties are the function of the milling conditions.

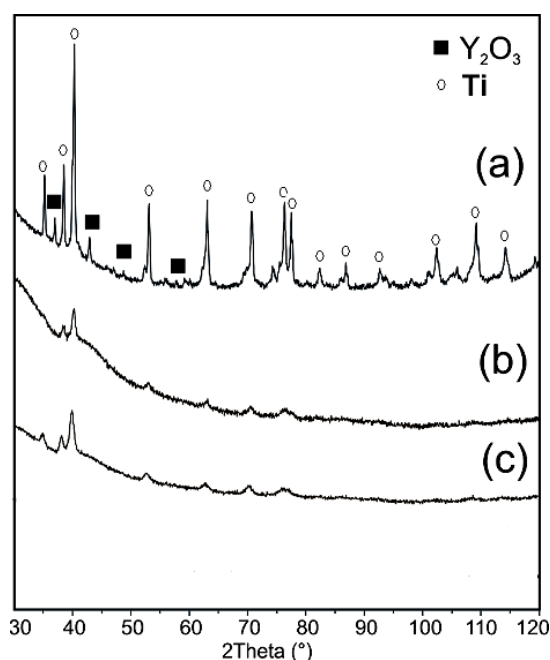


Figure 1. X-ray data for mixture of the microcrystalline Ti, and Y_2O_3 powder before MA (a) after MA for 24 h (b), and after MA for 48 h (c)

Figure 2 shows the SEM morphologies of the fabricated Ti-10wt% Y_2O_3 powder mixtures, at the various stages during milling and particle size distribution of the powder after milling. Figure 2a shows morphologies of the initial Ti-10wt% Y_2O_3 mixture before milling, it can be seen that the majority of the mixture powders are irregular. Also, it can be seen that after 6 h of milling, the powder shows inhomogeneous size distribution as shown in Fig. 2 b. With the increase of milling time, the size of the mixed powders decreases gradually and the microstructure is more homogeneous and becomes ultrafine, as shown in Fig. 2 c. After milling for 24 h, steady-state equilibrium is attained when a balance is achieved between the rate of welding, which tends to increase the average particle size, and the rate of fracturing, which tends to decrease the average composite particle size. Smaller particles are able to withstand deformation without fracturing and tend to be welded into larger pieces, with an

overall tendency to drive both very fine and very large particles towards an intermediate size. At this stage each particle contains substantially all of the starting ingredients, in the proportion they were mixed together and the particles reach saturation hardness due to the accumulation of strain energy. The particle size distribution at this stage is narrow, because particles larger than average are reduced in size at the same rate that fragments smaller than average grow through agglomeration of smaller particles

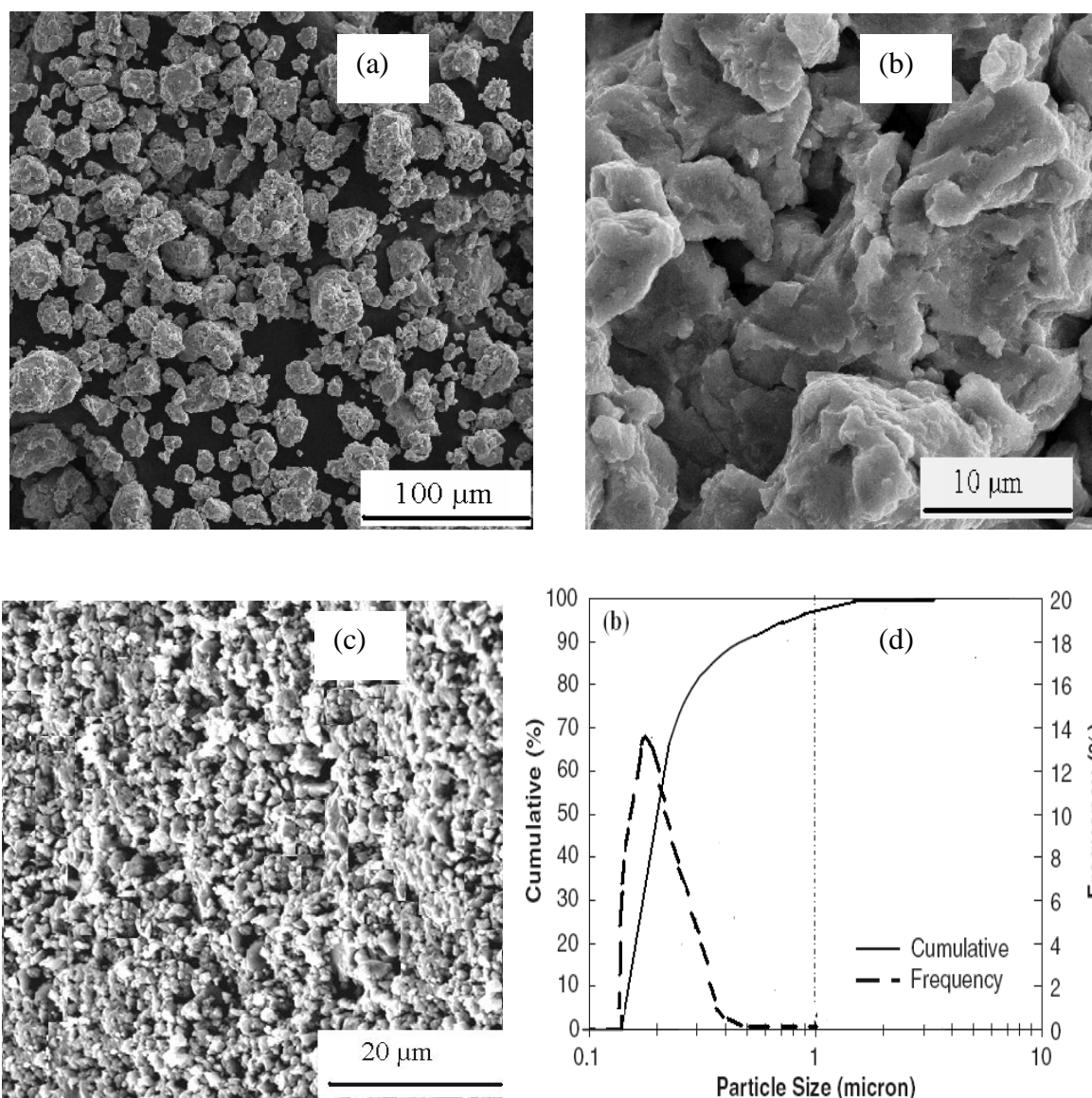


Figure 2. SEM images show morphologies of powder mixtures of Ti-10w% Y_2O_3 composite at the various stages during milling: (a) at 0 h, (b) at 6 h, (c) at 24 h. (d) particle size distribution after milling.

Figure 2 d shows the particle size distribution of the powder measured using Microtrac UPA150 (Montgomeryville, PA). It can be seen that the particle size of the powder after were reduced and the average particle size became 150 nm.

The microstructure of milled Ti-Y₂O₃ powder was studied by TEM. The TEM micrograph and corresponding selected area diffraction (SAD) pattern of the samples milled for 24 h is shown in Fig. 3. The TEM picture of the powder containing 10 wt.% Y₂O₃ suggests the formation of an amorphous phase. Apart from prevailing amorphous phase, the milled powders contained small amount of fine-crystalline (not shown). Lack of any sharp reflections in the XRD pattern, as shown in Fig. 1c, suggests that the amount of the crystalline phase is very low. There is a competition between the formation of an amorphous phase and the precipitation of crystallites. Apparently, when that Gibbs free energy of the amorphous phase is lower than that of the crystallites, solid-state amorphization takes place during MA. The amorphization reaction can be explained by high energies given to the powders during milling. The severe plastic deformation and extreme structural refinement, which have occurred during milling, increase the density of defects and the constraint of the neighboring crystallites [18], thereby decreasing the stability of the crystalline structure and promoting amorphization.

Formation of the compacts of nanocomposites was achieved by cold uniaxial pressing at relatively low pressure to get a compact with high porosity. The sintering results in compacts, used for the next treatment, respective for the pores formation. Due to the large volume of the grain boundaries, which state the easy paths for the electrolyte penetration, the compacts with relatively low density (85% of the theoretical density) are attractive material for the electrochemical etching. For this reason the nanocomposite compacts were etched fast and easy. After electrochemical etching, the nanocomposite compacts achieved density of about 80% of the bulk ingots, which is related to pores in the compacts.

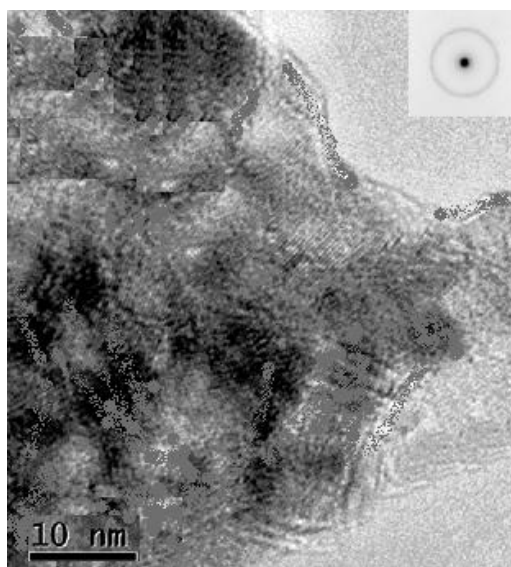


Figure 3. TEM micrograph and corresponding SAD patterns of the powder Ti-10wt.% Y₂O₃

The advantage of ultrafine structure and electrochemical etching that they are playing a key role for the surface modification. During electrochemical etching process the electrolyte penetrates mainly of the grain boundaries, resulting in the grains removing and pores formation. In this process,

conducted at relatively low anodic voltage, the surface is essentially improved by the oxidizing. This treatment (pores formation) results in attraction for corrosion resistance oxide formation and for tissue fixing surface roughening. The rough surface of the etched alloys is promising for implants for hard tissue replacements. The pores act as the anchors for the growing tissue and fixing them inside the pores.

The morphology of the samples after sintering and additional electrochemical etching (Fig. 4) was investigated by SEM. The porosity remaining after sintering is well visible as can be seen in Fig. 4 a and b. The etched surface of the nanocomposite alloys is very rough with pore diameter of up to 40 μm (Fig. 4a).

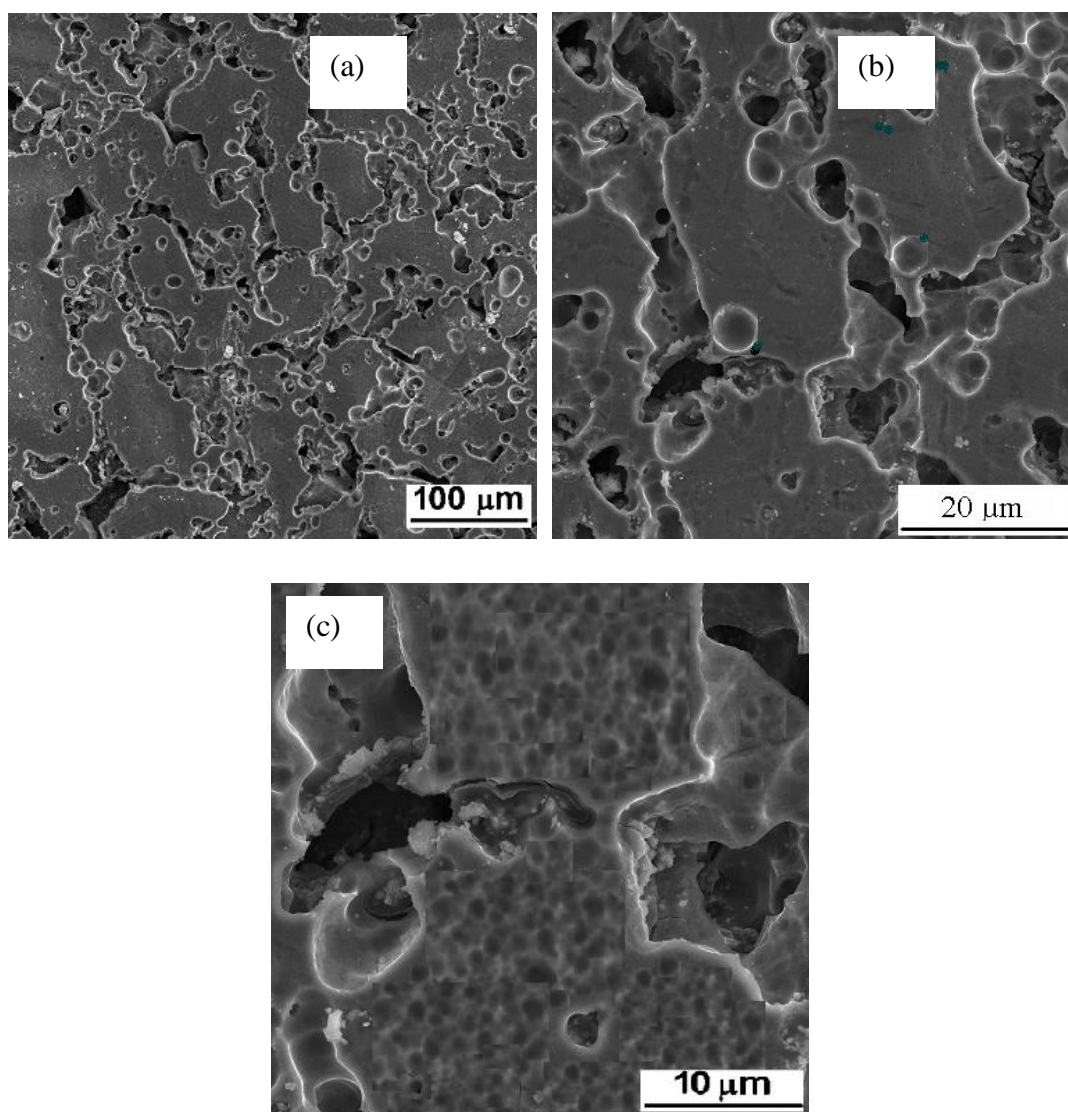


Figure 4. SEM images show morphologies of powder mixtures of Ti–10 wt.% Y_2O_3 composite, a) before electrochemical etching, b) before electrochemical etching with another magnification, c) after electrochemical etching.

Larger magnification and closer inspection of the porous nanocomposite sinters reveal that the remaining relatively flat topmost surface layer is also etched, with achieved pore diameter of about 0.1–2 μm (Fig. 4c). The compacts with relatively low density (85% of the theoretical density) are attractive material for the electrochemical etching, due to the large volume of the grain boundaries, which state the easy paths for the electrolyte penetration. For that reason the nanocomposite compacts were etched fast and easy. The applied electrolyte contained H_3PO_4 with small HF addition, which enhanced dissolution and results in porous Ti- Y_2O_3 compacts (Fig. 4c). After pressing, sintering and electrochemical etching, the nanocomposite compacts achieved density of about 80% of the bulk ingots, which is related to pores in the compacts.

Figure 5 shows the effect of addition Y_2O_3 to Ti, mechanical alloying, and electrochemical etching on the hardness of the composite. It is worth to notice that the values of hardness present a tendency to increase with addition Y_2O_3 for compacted at microcrystal or at nanocomposite. In addition the hardness increases dramatically after mechanical alloying.

The increase in hardness with alloying time at 24 h is due, possibly, to the increased formation of intermetallics causing a solid solution strengthening effect. The Y_2O_3 could be partially dissolved in the matrix and provide O_2 , to form titanium oxide, a very hard phase. Y element in Y_2O_3 may also react with Ti to form titanium yteria under certain conditions, which is also a hard phase. Also, it can be noticed that the hardness increases after electrochemical etching. Hardness is regarded as an indicative of wear resistance [14].

The corrosion resistance was investigated in simulated body fluids using potentiodynamic method. The polarization curves of microcrystalline Ti- Y_2O_3 and nanocomposites Ti- Y_2O_3 before and after electrochemically etching are shown in Fig 6. The polarization data obtained for sintered composites and microcrystalline titanium, including corrosion potentials (E_c), and corrosion current densities (I_c) values are summarized in Table 1. From this table it is possible to observe that Y_2O_3 doped to Ti had a positive effect on corrosion resistance of Ti after electrochemical etching. The corrosion test results indicate that the microcrystalline Ti possesses lower corrosion resistance and thus higher corrosion current density ($I_c = 1.52 \times 10^{-5} \text{ A/cm}^{-2}$) in Ringer's solutions.

The decrease in anodic current was greater than that in the cathodic current. Cathodic Tafel slopes, b_c , showed no visible trends, fluctuating between -221 and -245 mV/dec, while anodic Tafel slopes, b_a , increased from approximately 370 to 398 mV/dec. This indicated that the transfer of electrons became more difficult from anodic sites. The polarization curves of these nanocomposites had wider passive region which can provide excellent corrosion resistance. Besides, the reinforced Y_2O_3 with Ti decreased about hundredfold the corrosion rate of Ti. The corrosion resistant of titanium is a very important factor for biomedical applications and the corrosion behavior investigated in Ringer's solution on Ti-10 wt% Y_2O_3 nanocomposite show that the porous layer has lower corrosion current and the oxide layer is more stable with comparison with pure Ti with native oxide [19].

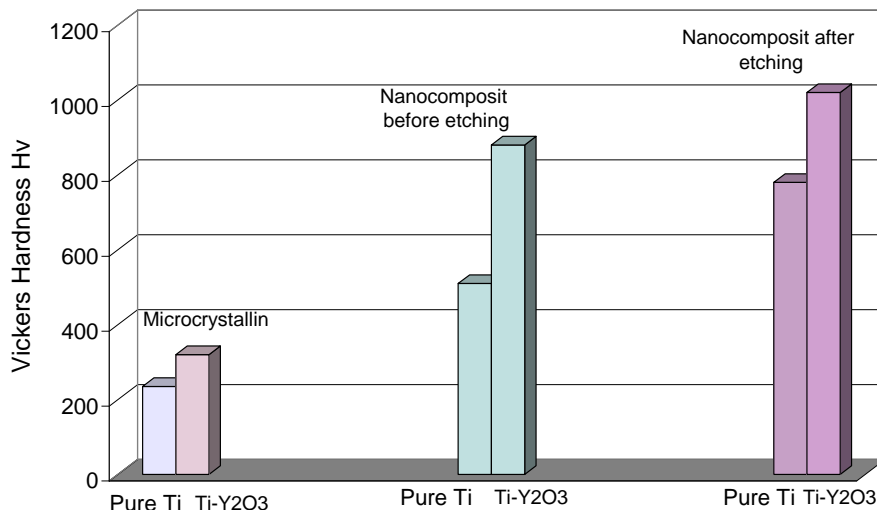


Figure 5. Influence of Y₂O₃ addition, mechanical alloying, and electrochemical etching on hardness of the Ti-Y₂O₃ nanocomposites

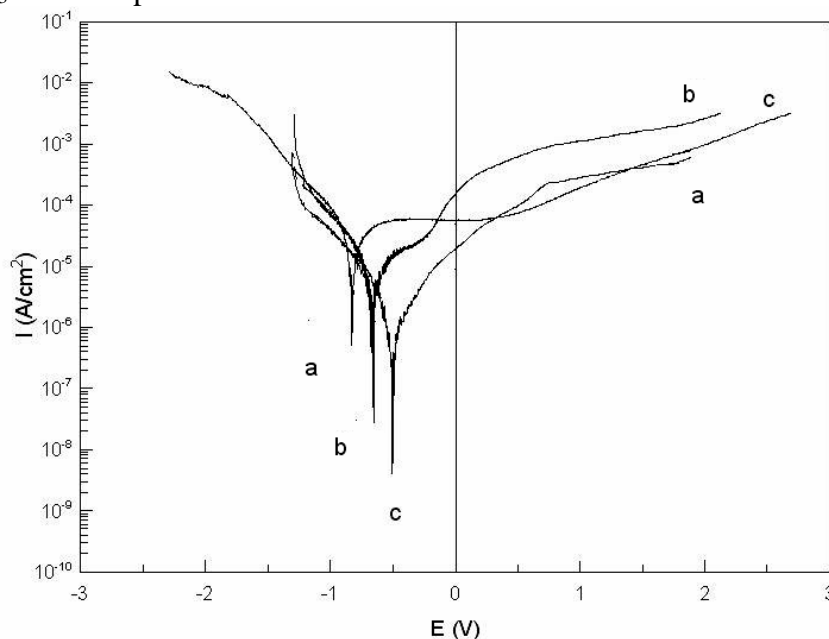


Figure 6. Potentiodynamic polarization curves of: (a) pure Ti microcrystalline, (b) Ti-10 w% Y₂O₃ nanocrystalline not etched, and (c) Ti-10 w% Y₂O₃ nanocrystalline etched composites in Ringer’s solution.

Table 1. Corrosion results for pure Ti microcrystalline and T-Y₂O₃ nanocrystalline before and after etching

Composition	I _{corr} (A/cm ²)	E _{corr} (V)	Tafel slopes	
			b _a (mV/dec)	b _c (mV/dec)
Ti pure microcrystalline	1.52×10 ⁻⁵	-0.78	370	-221
Ti-10% Y ₂ O ₃ nanocrystalline not etched	7.51×10 ⁻⁵	-0.61	385	-232
Ti-10% Y ₂ O ₃ nanocrystalline etched	9.15×10 ⁻⁶	-0.52	398	-245

4. CONCLUSION

In this study, the structure, mechanical and corrosion properties of Ti-Y₂O₃ nanocomposites synthesized by mechanical alloying, powder metallurgical and electrochemical etching processes were studied. This study provided the first evidence of an enhancement of the properties due to the nanoscale structures in consolidated Ti-Y₂O₃ materials. The studies lead to the following conclusions.

1- Nanostructured Ti-Y₂O₃ composites possess greater Vicker's hardness compared with microcrystalline titanium, and the electrochemical etching of the Ti-Y₂O₃ nanocomposites results in greater Vicker's hardness compared to non electrochemical etching of samples

2- The Ti-Y₂O₃ nanocomposites are more corrosion resistant than the microcrystalline Ti-Y₂O₃.

3- Electrochemical etching of the Ti-Y₂O₃ nanocomposites results in microporous surface. The prepared porous ultrafine alloys could be possible candidate for hard tissue implant applications, where the pores will improve bonding with the bone.

ACKNOWLEDGEMENTS

The authors would like to extend their sincere appreciation to the Deanship of Scientific Research at King Saud University for its funding this Research Group NO. (RG 1435-001)

References

1. D.M. Brunette, P. Tengvall, M. Textor, P. Thomsen (Eds.), Springer, Berlin, Heidelberg, New York, Tokyo, (2001).
2. O. Adamopoulos, T.J. Papadopoulos, *J. Mater. Sci.: Mater. Med.* 18 (2007) 1587.
3. H.N. Liu, T.J. Webster, *Biomaterials* 28 (2007) 354.
4. J. Jakubowicz, G. Adamek, *Electrochemistry Communications* 11 (2009) 1772–1775
5. M. Long, H.J. Rack, *Biomaterials* (1998); 19: 1621–1639.
6. R. Narayanan, S.K. Seshadri, *Corros. Sci.* 49 (2007); 542–558.
7. M. Niinomi, *Sci. Technol. Adv. Mater.* (2003), 4, 445–454.
8. M. Niinomi, *Biomaterials* 24 (2003) 2673–2683
9. S.R. Bhattarai, K.A. Khalil, M. Dewidar, P.H. Hwang, H.K. Yi, H.Y. Kim, *J of Biomedical Mater Research: Part A*, Vol. 86A,2, (2007) 289–299.
10. G. Adamek, J. Jakubowicz, *Materials Chemistry and Physics* 124 (2010) 1198–1204.
11. Dirk Handtrack, F. Despang, C. Sauer, B. Kieback, N. Reinfried, Y. Grin, *Materials Science and Engineering A* 437 (2006) 423–429.
12. Yuhua Li, Chao Yang, Haidong Zhao, Shengguan Qu, Xiaoqiang Li and Yuanyuan Li, *Materials*, 7, (2014), 1709–1800.
13. K. Niespodziana, K. Jurczyk, J. Jakubowicz, M. Jurczyk, *Materials Chemistry and Physics* 123 (2010) 160–165.
14. M. Dewidar, *Materials & Design* 31, (2010), 3964–3970.
15. H. Ruihua, M. Dewidar, J.K. Lim, *J Mater Sci Technol*, (2007); 23: 257–261.
16. J. Danie, I. Jorgensen, David C. Dunand, *Acta Materialia* 59 (2011) 640–650.
17. C. Suryanarayana, *Progress in Materials Science* 46 (2001) 1–184

18. R. Amini, M.J. Hadianfard, E. Salahinejad, M. Marasi, T. Sritharan, *J. Mater. Sci.* 44 (2009) 136-148.
19. J. Jakubowicz, *Electrochemistry Communications* 10 (2008) 735–739

© 2014 The Authors. Published by ESG (www.electrochemsci.org). This article is an open access article distributed under the terms and conditions of the Creative Commons Attribution license (<http://creativecommons.org/licenses/by/4.0/>).